Tryptophan-independent auxin biosynthesis contributes to early embryogenesis in *Arabidopsis*

Bing Wang[a,1], Jinfang Chu[b,1], Tianying Yu[a,1], Qian Xu[a], Xiaohong Sun[b], Jia Yuan[a], Guosheng Xiong[a], Guodong Wang[a], Yonghong Wang[a,b], and Jiayang Li[a,b,2]

[a]State Key Laboratory of Plant Genomics and [b]National Center for Plant Gene Research (Beijing), Institute of Genetics and Developmental Biology, Chinese Academy of Sciences, Beijing 100101, China

Contributed by Jiayang Li, February 27, 2015 (sent for review February 5, 2015; reviewed by Klaus Palme and Hong-Wei Xue)

The phytohormone auxin regulates nearly all aspects of plant growth and development. Tremendous achievements have been made in elucidating the tryptophan (Trp)-dependent auxin biosynthetic pathway; however, the genetic evidence, key components, and functions of the Trp-independent pathway remain elusive. Here we report that the *Arabidopsis indole synthase* mutant is defective in the long-anticipated Trp-independent auxin biosynthetic pathway and that auxin synthesized through this spatially and temporally regulated pathway contributes significantly to the establishment of the apical–basal axis, which profoundly affects the early embryogenesis in *Arabidopsis*. These discoveries pave an avenue for elucidating the Trp-independent auxin biosynthetic pathway and its functions in regulating plant growth and development.

phytohormone | IAA biosynthesis | tryptophan | embryogenesis | *Arabidopsis thaliana*

The phytohormone auxin plays critical roles in almost every aspect of plant development including embryogenesis, architecture formation, and tropic growth. One of the most fascinating topics in plant biology is how auxin can have so many diverse and context-specific functions (1). Dynamic auxin gradients, which are regulated mainly by local auxin synthesis, catabolism, conjugation, and polar auxin transport, are essential for integration of various environmental and endogenous signals (2, 3). Auxin perception and signaling systems are responsible for a read-out of the auxin gradients (1).

Local auxin biosynthesis is important for leaf development, shade avoidance, root-specific ethylene sensitivity, vascular patterning, flower patterning, and embryogenesis (4). Indole-3-acetic acid (IAA), the naturally occurring principal auxin in plants, is biosynthesized from tryptophan (Trp) through four proposed routes according to their key intermediates, namely indole-3-acetaldoxime (IAOx), indole-3-pyruvic acid (IPyA), indole-3-acetamide (IAM), and tryptamine (TAM) (5). The TRYPTOPHAN AMINOTRANSFERASE OF ARABIDOPSIS (TAA)/YUCCA (YUC) linear pathway has been considered as a predominant Trp-dependent auxin biosynthetic pathway (4, 6–8). However, labeling studies and analyses of Trp auxotrophic mutants have long predicted the existence of a Trp-independent IAA biosynthetic pathway (9–13). When the *Arabidopsis* and maize seedlings were fed with isotope-labeled precursor, IAA was more enriched than Trp, and the incorporation of label into IAA from Trp is low, suggesting that IAA can be produced de novo without Trp as an intermediate (11, 12). The Trp biosynthetic mutant *trp1*, defective in phosphoribosylanthranilate transferase (PAT), and indole-3-glycerol phosphate synthase (IGS) antisense plants are deficient in steps earlier than indole-3-glycerol phosphate (IGP) formation and display decreased levels of both IAA and Trp (10, 14). However, the *trp3* and *trp2* mutants, defective in tryptophan synthase α (TSA) and tryptophan synthase β (TSB) subunits, respectively, accumulate higher levels of IAA than the wild type despite containing lower Trp levels (10, 11, 15, 16). These data strongly suggested the existence of the Trp-independent IAA biosynthetic pathway that might branch from IGP and/or indole (10). Further studies suggested that a cytosol-localized indole synthase (INS) may be involved in the Trp-independent biosynthesis of indole-containing metabolite (17). However, the molecular basis, biological functions, and spatiotemporal regulation of the Trp-independent IAA biosynthetic pathway have remained a mystery.

In higher eukaryotes, embryogenesis initiates the generation of the species-specific body plan. During embryogenesis, a single-celled zygote develops into a functional multicellular organism with cells adopting specific fates according to their relative positions. In higher plants, essential architecture features, such as body axes and major tissue layers, are established in embryogenesis, and auxin plays a vital role in apical-basal patterning and embryo axis formation (18, 19). Local auxin biosynthesis, polar auxin transport facilitated by PIN-FORMED1/3/4/7 (PIN1/3/4/7), and auxin response coordinately regulate apical–basal pattern formation during embryogenesis (7, 20–22). The TAA and YUC families in Trp-dependent IAA biosynthesis predominantly regulate embryogenesis at or after the globular stage (7, 22). However, the auxin source for embryogenesis before the globular stage remains elusive. In this study, we provide, to our knowledge, the first genetic and biochemical evidence that the cytosol-localized INS is a key component in the long predicted Trp-independent auxin biosynthetic pathway and is critical for apical–basal pattern formation during early embryogenesis in *Arabidopsis*.

Significance

The phytohormone indole-3-acetic acid (IAA) plays a vital role in plant growth and development. IAA can be synthesized through the precursor tryptophan (Trp), known as the Trp-dependent IAA biosynthetic pathway. However, IAA may also be synthesized through a proposed Trp-independent IAA biosynthetic pathway. Although the Trp-independent IAA biosynthesis was hypothesized 20 years ago, it remains a mystery. In this paper, we provide compelling evidence that the cytosol-localized indole synthase (INS) initiates the Trp-independent IAA biosynthetic pathway and that the spatial and temporal expression of INS plays an important role in the establishment of the apical–basal pattern during early embryogenesis, demonstrating that the Trp-dependent and -independent IAA biosynthetic pathways coordinately regulate embryogenesis of higher plants.

Author contributions: J.L. supervised the project; B.W., J.C., T.Y., and J.L. designed research; B.W., J.C., T.Y., Q.X., X.S., J.Y., G.X., and G.W. performed research; B.W., J.C., T.Y., and J.L. analyzed data; and B.W., Y.W., and J.L. wrote the paper.

Reviewers: K.P., Albert Ludwigs University of Freiburg; and H.-W.X., Institute of Plant Physiology and Ecology, Shanghai Institutes of Biological Sciences, Chinese Academy of Sciences.

The authors declare no conflict of interest.

Freely available online through the PNAS open access option.

[1]B.W., J.C., and T.Y. contributed equally to this work.

[2]To whom correspondence should be addressed. Email: jyli@genetics.ac.cn.

This article contains supporting information online at www.pnas.org/lookup/suppl/doi:10.1073/pnas.1503998112/-/DCSupplemental.

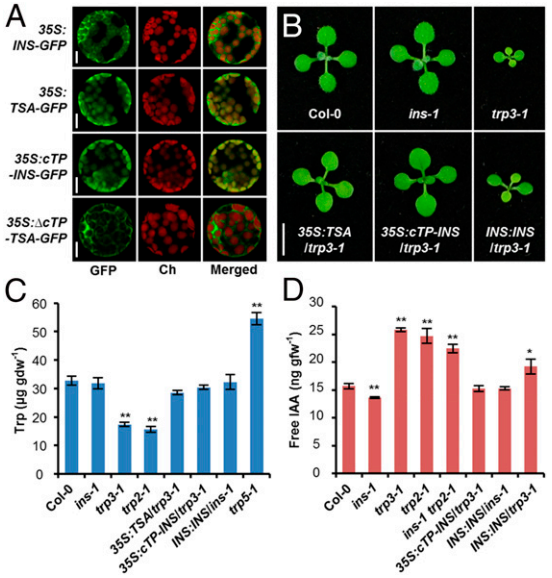

Fig. 1. INS and TSA display distinct subcellular localizations and different functions in tryptophan biosynthesis and IAA biosynthesis. (*A*) Subcellular localizations of INS-GFP, TSA-GFP, cTP-INS-GFP, and ΔcTP-TSA-GFP in protoplasts from stable transgenic plants. Ch, chlorophyll. (*B*) Phenotypes of 12-d-old wild-type (Col-0), *ins-1*, *trp3-1*, *35S:TSA/trp3-1*, *35S:cTP-INS/trp3-1*, and *INS:INS/trp3-1* seedlings. (*C*) Tryptophan (Trp) contents in 7-d-old seedlings. gdw^{-1}, per gram dry weight. The Trp accumulation mutant *trp5-1* was used as a control. Data are represented as mean ± SEM; $^{**}P < 0.01$ by Student's *t* test; $n = 5$. (*D*) Free IAA contents in 12-d-old seedlings ($n = 5$). gfw^{-1}, per gram fresh weight. Data are represented as mean ± SEM; $^{*}P < 0.05$ and $^{**}P < 0.01$ by Student's *t* test; $n = 5$. (Scale bars, 10 μm in *A* and 0.5 cm in *B*.)

Results

Functional Differentiation of INS and TSA Results from Their Distinct Subcellular Localizations. INS and TSA are close paralogs that contain a conserved Trp synthase α-subunit domain (Fig. S1*A*). TSA contains a chloroplast transit peptide (cTP) domain and is localized in chloroplasts, whereas INS lacks the cTP and is localized in cytosol in protoplasts of stable transgenic plants (Fig. 1*A*). Trp biosynthesis has been proposed to take place in chloroplasts, and TSA and TSB were considered to form a complex and catalyze the formation of Trp (10, 23, 24). Previous work has shown that INS could complement Trp auxotrophy of the *Escherichia coli Δtrp A* strain, which is defective in Trp biosynthesis due to the deletion of TSA (17). We therefore investigated whether INS participates in IAA biosynthesis through the Trp-independent pathway. Based on the findings that both *trp3-1* and *trp2-1* mutants, defective in *TSA* and *TSB1*, respectively, are Trp auxotrophic (15, 16), we show here that they have lower contents of Trp, whereas the *INS* null mutant shows little Trp auxotrophic phenotype and has a normal Trp content (Fig. 1 *B* and *C* and Fig. S1). Overexpression of *INS* with a *cTP* (*cTP-INS*) could completely rescue the Trp auxotrophic phenotype and restore the Trp level of *trp3-1*, whereas overexpression of *INS* could only partially rescue *trp3-1* (Fig. 1 *B* and *C* and Fig. S2), suggesting that INS could produce indole in cytosol and feed into Trp biosynthesis effectively if relocated to the chloroplast. Furthermore, the *trp3-1* and *trp2-1* mutants have higher levels of IAA than the wild type, whereas the *INS* null mutants *ins-1* and *ins-2* have decreased IAA levels (Fig. 1*D* and Fig. S1 *C–E*). *INS* could complement the deficiency of *ins-1* in terms of the IAA content and *DR5*-driven GUS activity that reflects the read-out of auxin signal transduction (25), suggesting that INS is involved in auxin biosynthesis (Fig. 1*D* and Fig. S3*A*). Overexpression of *cTP-INS* could restore the IAA level of *trp3-1*, whereas overexpression of *INS* could only partially rescue *trp3-1* (Fig. 1*D*). Overexpression of *TSA* without a *cTP* (*ΔcTP-TSA*) could rescue *DR5*-driven GUS activities in cotyledons of *ins-1*, whereas *TSA* or *cTP-INS* overexpression had only a partial effect (Fig. S3*A*). Collectively, these data demonstrate that functional differentiation of INS and TSA results from their distinct subcellular localizations.

We then investigated the effect of exogenous Trp on phenotypes and IAA levels of wild type, *ins-1*, and *trp3-1*. Treatment of *trp3-1* with Trp could largely restore the disordered expression pattern of *DR5:GUS* on root tips and root growth and reduce the IAA accumulation (from 67 to 36% above the wild type) (Fig. S3 *B–D*). However, Trp could not fully restore the *DR5:GUS* pattern nor raise the IAA level in *ins-1* compared with that in the wild type (Fig. S3 *B–D*), consistent with the hypothesis that INS participates specifically in the Trp-independent IAA biosynthetic pathway.

INS Specifically Participates in the Trp-Independent IAA Biosynthesis. To further distinguish the activities of Trp-dependent and -independent IAA biosynthetic pathways, seedlings of Columbia (Col-0), *ins-1*, and *trp3-1* were treated with labeled anthranilic acid in the presence or absence of unlabeled Trp at high temperature and then the labeled IAA contents were measured (Fig. 2*A* and Fig. S4 *A* and *B*). Anthranilic acid is a common precursor of the Trp-dependent and -independent IAA biosynthetic pathways, whereas exogenous Trp should increase the Trp pool size

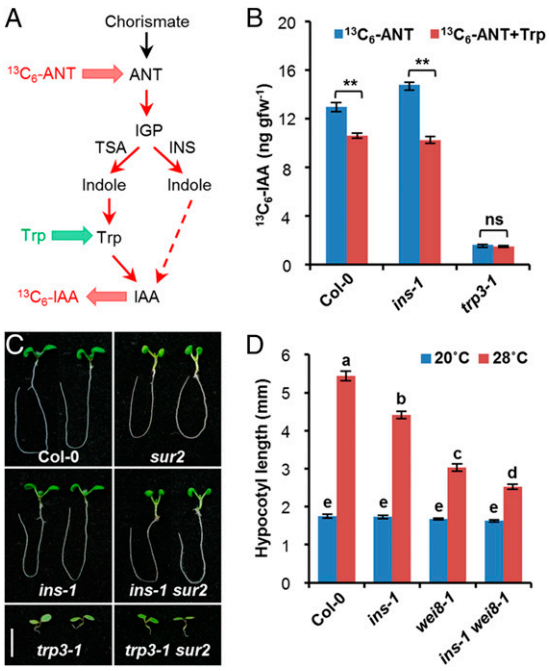

Fig. 2. INS is a key component in the Trp-independent IAA biosynthetic pathway. (*A*) Schematic diagrams of $^{13}C_6$-anthranilic acid ($^{13}C_6$-ANT) feeding experiment. Seedlings were transferred to liquid Murashige and Skoog (MS) media containing $^{13}C_6$-ANT and cultured for 24 h. In a parallel test, the MS media contained $^{13}C_6$-ANT and unlabeled Trp, which should increase the Trp pool size and decrease the biosynthesis of $^{13}C_6$-IAA only through the Trp-dependent pathway. (*B*) $^{13}C_6$-IAA contents in 12-d-old wild-type (Col-0), *ins-1*, and *trp3-1* seedlings after $^{13}C_6$-ANT or $^{13}C_6$-ANT plus Trp treatment. gfw^{-1}, per gram fresh weight; ns, no significant difference. Data are represented as mean ± SEM; $^{**}P < 0.01$ by Student's *t* test; $n = 5$. (*C*) Phenotypes of 7-d-old wild-type (Col-0), *ins-1*, *sur2*, *ins-1 sur2*, *trp3-1*, and *trp3-1 sur2* seedlings. (Scale bar, 0.5 cm.) (*D*) Hypocotyl length of 9-d-old wild-type (Col-0), *ins-1*, *wei8-1*, and *ins-1 wei8-1* seedlings at 20 °C and 28 °C. Data are represented as mean ± SEM; different letters indicate significant difference by Tukey's multiple comparison test ($P < 0.05$); $n = 30$.

and decrease the biosynthesis of $^{13}C_6$-IAA through the Trp-dependent pathway (Fig. 2*A*). When exogenous Trp was applied, the wild-type and *ins-1* seedlings exhibited significant decreases in the $^{13}C_6$-IAA content, but this was greater in *ins-1* (31%) compared with that of the wild type (18%), whereas *trp3-1* seedlings displayed no significant decrease (Fig. 2*B*), indicating that Trp-independent IAA biosynthesis was deficient in *ins-1* whereas Trp-dependent IAA biosynthesis was impaired in *trp3-1*. These phenomena explain the defective root development of *trp3-1*, such as reduced main root length and impaired gravitropism (Fig. S3*C*), which resemble the root phenotypes of *wei8-1 tar2-1* and *wei8-1 tar2-2 tar1-1* seedlings (7). Consistent with this, we found that the high-auxin phenotypes such as the elongated hypocotyl and extended petiole of *sur2*, in which the Trp-dependent IAA biosynthesis is elevated (26), were suppressed by *trp3-1* but not by *ins-1* (Fig. 2*C* and Fig. S4*C*). And the *trp3-1 sur2* double mutant displayed similar Trp auxotrophic phenotypes to *trp3-1* (Fig. 2*C* and Fig. S4*C*). Furthermore, we found that the *ins-1* mutant is impaired in the hypocotyl elongation induced by high temperature and has an additive effect with *wei8-1* (Fig. 2*D*), a null mutant of *TAA1* in the Trp-dependent IAA biosynthetic pathway (7), suggesting that INS probably acts in a parallel pathway with TAA1 to regulate the hypocotyl length at high temperature. Taken together, these results indicate that INS is involved in the production of IAA through the Trp-independent pathway.

INS Is Required for Early Embryogenesis. In *Arabidopsis* the cell division pattern of an embryo is nearly stereotypic. In the wild type, a zygote divides asymmetrically, generating a smaller apical cell and a larger basal cell. The apical cell undergoes two rounds of longitudinal, one round of horizontal, and one round of periclinal divisions, giving rise to a 16-cell embryo proper, whereas the basal cell divides transversely to produce the suspensor (18). The uppermost suspensor cell is specialized to the hypophysis (HY), which subsequently produces an upper lens-shaped cell (LSC) that will form the quiescent center (QC) and a lower daughter cell that will form the columella stem cells (CSC) (Fig. 3*A* and Fig. S5*A*). The embryo development of *trp3-1* is normal (Fig. 3*B*); however, the stereotypical pattern of cell division is disturbed in *ins-1* from the one-cell stage onward (Fig. 3 *C–I*). In both *ins-1* and *ins-2* mutants, ~6–9% embryos arrested at the 1-, 4-, 8-, or 16-cell stage with a correct cell division pattern (Fig. 3*C* and Fig. S5 *B*, *M*, and *O*), and more importantly, ~11–14% embryos displayed abnormal cell division patterns (Fig. 3 *D–I* and Fig. S5 *C–M* and *O*). For example, the apical cell, basal cell, and their progeny underwent divisions with abnormal cell plates at a wrong position or in a wrong orientation (Fig. 3 *D–G* and Fig. S5 *C–F*, arrow). From the globular to torpedo stages, the cell group in the basal embryo region, which normally displays characteristic cell arrangement, was consistently disorganized (Fig. 3 *G–I* and Fig. S5 *G–L*, bracket). Furthermore, there is no cotyledon primordium bulging out in the apical embryo region (Fig. 3*I* and Fig. S5*L*). The embryonic defects could be complemented by overexpression of the wild-type *INS* gene (Fig. S5 *N* and *O*), demonstrating that *INS* is responsible for the defective embryogenesis of *ins-1*. Together, it is suggested that *INS* plays a critical role in early embryogenesis.

Furthermore, we can identify neither an *ins-1 trp3-1* seedling from more than 500 progeny of the *ins-1 trp3-1*$^{+/-}$ plants nor an *ins-1 trp3-100* seedling from more than 500 progeny of the *ins-1 trp3-100*$^{+/-}$ plants, indicating that the *ins-1 trp3-1* and *ins-1 trp3-100* double mutants were completely embryo lethal. Both *ins-1 trp3-1* and *ins-1 trp3-100* exhibited arrested embryos with normal apical–basal polarity (Fig. 3*J* and Fig. S6 *A–D*) and embryos with abnormal cell division planes (Fig. 3 *K–P* and Fig. S6 *E–O*). These abnormal divisions resulted in embryos defective in the apical–basal polarity (Fig. 3 *K–N* and Fig. S6 *E–J*), embryos with disorganized basal cell regions (Fig. 3 *O* and *P* and Fig. S6 *K–O*), and embryos without cotyledon primordia (Fig. 3*P* and Fig. S6*O*). Occasionally, the *ins trp3* embryo formed filamentous structure without differentiation of the apical cell (Fig. 3*K* and

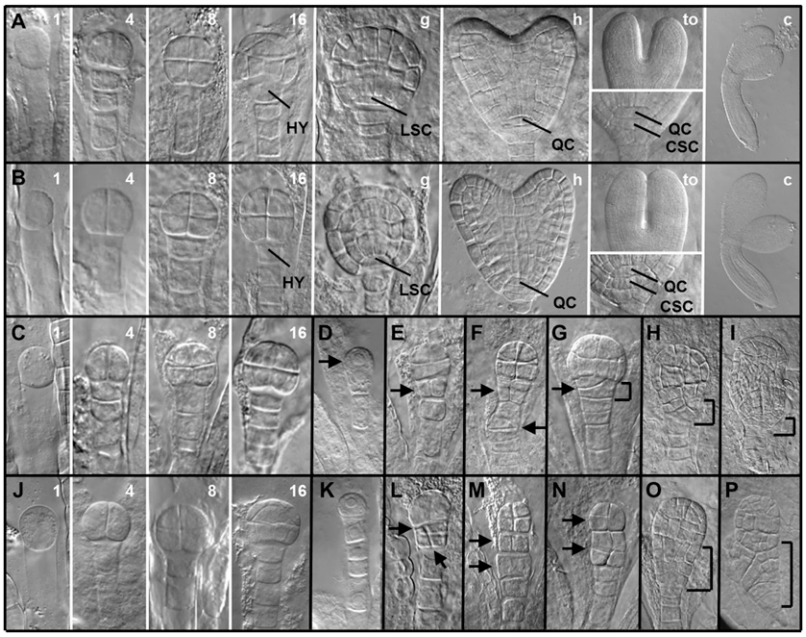

Fig. 3. Effects of INS and TSA on embryogenesis. Embryos of wild-type (Col-0) (*A*) and *trp3-1* (*B*) plants at 1-, 4-, 8- or 16-cell globular (g), heart (h), torpedo (to), and cotyledon (c) stages. HY, hypophysis; LSC, lens-shaped cell; QC, quiescent center; and CSC, columella stem cells. (*C–I*) When normal sibling embryos reach the heart stage, defective embryos of *ins-1* are arrested before the globular stage with normal body plans (*C*) or display abnormal cell division patterns (*D–I*). (*J–P*) When normal sibling embryos reach the heart stage, defective embryos from the *ins-1 trp3-1*$^{+/-}$ siliques are arrested with normal body plans (*J*) or exhibit abnormal cell division patterns (*K–P*). Arrows indicate aberrant cell divisions in early embryogenesis, and brackets mark aberrant basal cell regions.

Fig. S6*E*). The embryonic defects of *ins* and *ins trp3* resembled the defects of auxin-related mutants, such as *pin7*, *pin1/3/4/7*, *gnom*, *monopteros* (*mp*), and *bodenlos* (*bdl*) (20, 27–29), suggesting that deficiency in auxin activity is the likely cause of defects during early embryogenesis.

Trp-Independent IAA Biosynthesis Contributes to Apical–Basal Axis Establishment. To understand the roles of Trp biosynthesis and IAA biosynthesis in embryogenesis, we compared the embryo development of Col-0, *ins*, *trp3*, *ins trp3*, *trp2*, and *ins trp2* plants. The Trp auxotrophic mutants *trp3* and *trp2* underwent normal embryogenesis comparable to the wild type, whereas *ins-1* displayed a normal Trp level but a significantly higher percentage of defective embryos (Figs. 1*C*, 3*B*, and 4*A*; Fig. S7 *A–E*), suggesting that Trp biosynthesis may play a limited role in early embryogenesis. Furthermore, although *trp3-100* is a weak allele of *TSA* (15) (Fig. S1*A*), the *ins-1 trp3-100* double mutant is completely embryo lethal (Fig. 4*A* and Figs. S6 and S7 *A–E*), suggesting that *ins-1 trp3-1* and *ins-1 trp3-100* are embryo lethal probably because of a lack of auxin biosynthesis. Moreover, direct measurement of IAA contents in ovules showed that, compared with the wild type, free IAA levels decreased to 78% in morphologically normal ovules of *ins-1*, to 31% in morphologically abnormal ovules of *ins-1*, and to 15% in abnormal ovules of the *ins-1 trp3-1*$^{+/-}$ plants, whereas IAA levels increased to 115% in *trp3-1* ovules (Fig. 4*B*). Furthermore, we found that the embryonic deficiency of *ins-1* was suppressed by *trp2-1* and *trp2-301*, probably due to the increased IAA levels of *ins-1 trp2-1* and *ins-1 trp2-301* double mutants (Figs. 1*D* and 4*A*; Figs. S7 *A–E* and S8*A*), suggesting that IAA biosynthesis is important for early embryogenesis.

The Trp auxotrophic phenotypes of *ins-1 trp2-1* and *ins-1 trp2-301* were similar to those of *trp2-1* and *trp2-301*, respectively (Fig. S8*B*). These phenomena may be explained by the observation that *trp2-1* seedlings over-accumulated indole (11), which might diffuse from chloroplasts to the cytosol and compensate for the deficiency of *ins-1*.

We then compared the spatiotemporal expression patterns of INS and TSA proteins during embryogenesis. INS is expressed uniformly at the 1- and 2-cell stages, predominantly in suspensor cells at the 4- and 8-cell stages, and increases gradually in the proembryo, especially in the periphery and basal domains from the 16-cell stage. By contrast, TSA is expressed from the four-cell stage and exhibits a uniform expression pattern (Fig. 4*C*). The *DR5:GFP* reporter has been used to visualize the read-out of auxin signaling during embryogenesis (20, 30). We further compared the DR5 activity represented by GFP signals in Col-0, *ins-1*, *trp3-1*, and *ins-1 trp3-1* embryos. In the wild-type embryo, the GFP signals were observed in the apical cell and its progeny but very weakly in the suspensor cells before the globular stage (Fig. 4*D*). At the transition stages, GFP signals accumulated mainly at the root meristem region (Fig. 4*E*). Compared with the wild type, the *DR5:GFP* expression patterns were disturbed in arrested or morphologically defective *ins-1* embryos (Fig. 4 *F* and *G*), but displayed regular patterns in *trp3-1* (Fig. 4 *H* and *I*) and morphologically normal *ins-1* embryos (Fig. 4 *J* and *K*). In the *ins-1 trp3-1* embryos, the GFP signals were hardly detected in arrested embryos (Fig. 4*L*), nor in embryos with abnormal cell division patterns (Fig. 4*M*). Collectively, these results demonstrate that

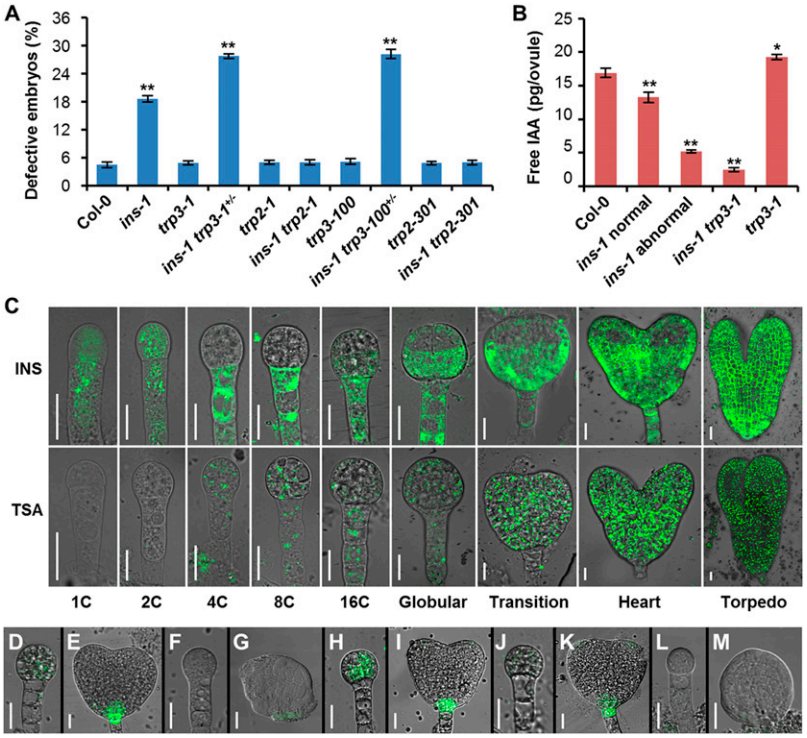

Fig. 4. Trp-independent IAA biosynthesis contributes significantly to early embryogenesis. (*A*) Percentage of defective embryos in the wild type (Col-0) and mutants at the globular stage. Data are represented as mean ± SEM; $^{**}P < 0.01$ by Student's *t* test; $n = 4$, and each biological repeat contains about 250 embryos. (*B*) Free IAA contents in ovules from the wild-type (Col-0), *ins-1*, *ins-1 trp3-1*$^{+/-}$, and *trp3-1* siliques. "*ins-1* normal" refers to the *ins-1* ovules with normal morphology, "*ins-1* abnormal" refers to the *ins-1* ovules containing defective embryos, and "*ins-1 trp3-1*" refers to the abnormal ovules from *ins-1 trp3-1*$^{+/-}$ siliques that contain defective embryos of *ins*, *ins trp3*$^{+/-}$, and *ins trp3-1*$^{-/-}$ together. Data are represented as mean ± SEM; $^{*}P < 0.05$ and $^{**}P < 0.01$ by Student's *t* test; $n = 5$. (*C*) Expression patterns of INS and TSA proteins during embryogenesis. 1C, 2C, 4C, 8C, and 16C represent 1-, 2-, 4-, 8-, and 16-cell stages, respectively. (*D–M*) *DR5* activities shown by GFP signals in wild-type embryos (*D* and *E*), defective *ins-1* embryos (*F* and *G*), *trp3-1* embryos (*H* and *I*), normal *ins-1* embryos (*J* and *K*), and *ins-1 trp3-1* embryos (*L* and *M*). (Scale bars, 15 μm in *C–M*.)

the Trp-independent IAA biosynthetic pathway provides an important auxin source for the development of early embryogenesis.

INS and YUC Coordinately Regulate Embryogenesis. To further evaluate the roles of Trp-dependent and Trp-independent auxin biosynthetic pathways in embryonic development, we carried out genetic analyses using *ins-1* and the *yuc4 yuc6* double mutant (*yuc4/6*). Compared with the wild type (Fig. 5*A*), *ins-1* exhibited arrested embryos (Fig. 5 *B* and *C*) and embryos defective in apical–basal polarity (Fig. 5 *D–F*), whereas *yuc4/6* embryos displayed mild defects at the basal embryo pole (Fig. 5*G*). The *ins-1 yuc4/6* triple mutant displayed an additive negative effect on embryogenesis and IAA biosynthesis (Fig. 5 *H–N*; Fig. S7 *F* and *G*). It should be pointed out that both *ins-1* and *yuc4/6* formed more branches than wild type, and the *ins-1 yuc4/6* triple mutant displayed an additive promotion on shoot branching (Fig. S9). Together, it is suggested that INS and YUC4/6 cooperatively regulate embryo development and apical dominance through parallel and independent pathways.

Discussion

Although genetic and metabolic studies have clearly established the importance of the Trp-dependent IAA biosynthetic pathway, IAA has also been proposed to be synthesized from IGP and/or indole through a Trp-independent pathway, which remains to be substantiated from genetic, biochemical, and functional studies (9–11). In this study, we demonstrate that the cytosol-localized INS is a key component in the long-speculated Trp-independent IAA biosynthetic pathway and contributes significantly to the establishment of the apical–basal pattern.

Based on our findings in this work, we propose an updated model of IAA biosynthetic pathways (Fig. 6). In *Arabidopsis* Trp

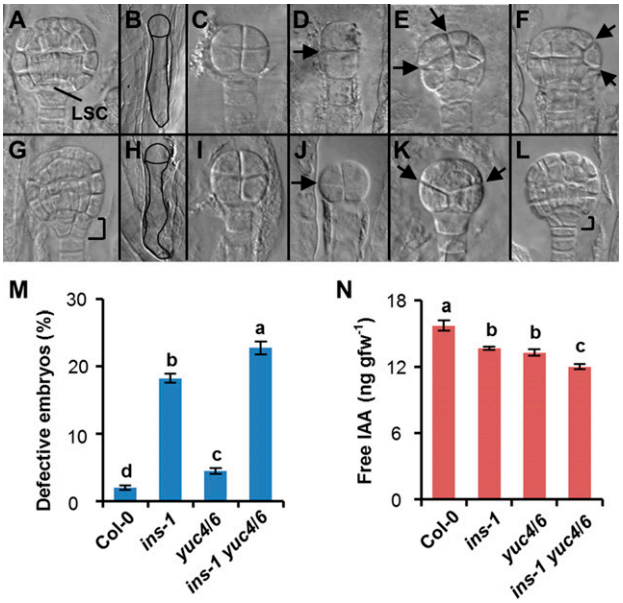

Fig. 5. INS and YUCs act in parallel IAA biosynthetic pathways. (*A–L*) Morphologies of wild-type (Col-0) (*A*), *ins-1* (*B–F*), *yuc4 yuc6* (*yuc4/6*) (*G*), and *ins-1 yuc4/6* (*H–L*) embryos at the globular stage. Arrows indicate aberrant cell divisions and brackets mark aberrant basal cell regions. (*M*) Percentage of defective embryos in Col-0, *ins-1*, *yuc4/6*, and *ins-1 yuc4/6* at the globular stage. Data are represented as mean ± SEM; different letters indicate significant difference by Tukey's multiple comparison test ($P < 0.05$); $n = 4$, and each biological repeat contains about 250 embryos. (*N*) Free IAA levels in 12-d-old Col-0, *ins-1*, *yuc4/6*, and *ins-1 yuc4/6* seedlings. gfw^{-1}, per gram fresh weight. Data are represented as mean ± SEM; different letters indicate significant difference by Tukey's multiple comparison test ($P < 0.05$); $n = 5$.

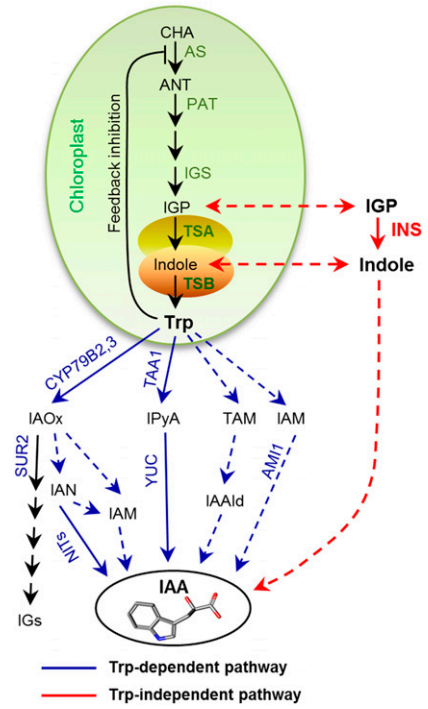

Fig. 6. A model of the Trp-dependent and Trp-independent IAA biosynthetic pathways. Solid arrows refer to pathways with identified enzymes and dashed arrows to undefined ones. ANT, anthranilate; AS, anthranilate synthase; CHA, chorismic acid; IAAld, indole-3-acetaldehyde; IAM, indole-3-acetamide; IAN, indole-3-acetonitrile; IAOx, indole-3-acetaldoxime; IGP, indole-3-glycerol phosphate; IGs, indole glucosinolates; IGS, indole-3-glycerol phosphate synthase; IPyA, indole-3-pyruvic acid; PAT, phosphoribosylanthranilate transferase; TAA1, tryptophan aminotransferase of Arabidopsis1; TAM, tryptamine; TSA, tryptophan synthase α; TSB, tryptophan synthase β; YUC, YUCCA.

biosynthesis takes place in chloroplasts, where TSA and TSB have been suggested to form a complex and convert IGP to Trp (10, 23, 24). The first step of Trp biosynthesis is catalyzed by anthranilate synthase (AS), which is a rate-limiting enzyme and subject to feedback inhibition by Trp (31). In the Trp-dependent pathway, IAA is biosynthesized through four proposed routes named after their key intermediates from the common precursor tryptophan, whereas, in the Trp-independent pathway, INS may mediate indole production in cytosol and initiate the Trp-independent IAA biosynthesis that plays an important role for apical–basal pattern formation during early embryogenesis. These two pathways coordinately regulate embryogenesis and apical dominance in *Arabidopsis*.

The $^{13}C_6$-anthranilic acid feeding experiment and genetic analysis between *trp3-1* and *sur2* indicate that the activity of Trp-dependent IAA biosynthesis is impaired in *trp3-1*. However, free IAA contents increase in *trp3-1* and *trp2-1*, probably due to impairment in Trp biosynthesis and release of the Trp feedback inhibition. Furthermore, the $^{13}C_6$-anthranilic acid feeding experiment and measurements of IAA contents in seedlings and ovules indicate that the Trp-independent IAA biosynthesis is dramatically impaired in *ins-1*, which produces ~18–22% defective embryos that are finally lethal during early embryogenesis. The *ins-1* seedlings with normal morphology should be generated from healthy embryos. The *ins-1 trp3-1* and *ins-1 trp3-100* double mutants are completely embryo lethal, most likely due to an impairment in both Trp-independent and -dependent auxin biosynthesis. However, the *ins-1 trp2-1* and *ins-1 trp2-301* double mutants display normal embryogenesis, similar IAA levels, and

PLANT BIOLOGY

comparable morphologies to *trp2-1* and *trp2-301*. These observations may be explained by the high levels of indole in *trp2* (11), which may diffuse from chloroplasts to the cytosol and compensate for the deficiency of *ins-1*. Similarly, in cytosol, INS converts IGP to indole, which may diffuse into chloroplasts and participate in Trp biosynthesis with a low efficiency. This explains why overexpression of *INS* can partially rescue *trp3-1* and why the *TSA* null mutant can survive under weak light conditions (15).

Our work has identified the source of auxin during early embryogenesis. In *Arabidopsis*, the early axis pattern is predominantly set up during early embryogenesis and provides the positional reference to postembryonic development (18). INS shows spatiotemporal expression patterns during embryogenesis and contributes to the establishment of an auxin gradient during embryogenesis. It is probable that local auxin biosynthesis through the Trp-independent and Trp-dependent pathways coordinately regulates the auxin gradient and orchestrates critical formative steps in the creation of apical–basal pattern during embryogenesis.

How indole is converted into IAA is a challenge. It will be interesting to investigate whether indole-3-butyric acid participates in the Trp-independent pathway (32). A systematic analyses of metabolic profiles of wild type, *ins-1*, and *trp3-1* treated with $^{13}C_6$-anthranilic acid and a large-scale genetic screening for embryo-lethal mutants in the *trp2* background may help to identify the key components in the Trp-independent IAA biosynthetic pathway. Further investigation of components and functions of this Trp-independent pathway will likely be an exciting area in the coming years.

Materials and Methods

Plant growth, plant transformation, and high-temperature–induced hypocotyl elongation were performed as previously described (33, 34). Free IAA content was measured in seedlings, aerial parts, and ovules as described previously (35, 36), with minor modifications in ultraperformance liquid chromatography-tandem mass spectrometer (UPLC-MS/MS) conditions. Primers used in this study are listed in Table S1. Details are provided in *SI Materials and Methods*.

ACKNOWLEDGMENTS. We thank the Arabidopsis Biological Resource Center for providing *ins-1* (SALK_138654), *trp3-1* (CS8331), *trp3-100* (CS8332), *trp2-1* (CS8327), *trp5-1* (CS8558), *tar2-1 wei8-1* (CS16414), and *sur2* (SALK_028573) seeds; the Nottingham Arabidopsis Stock Centre for providing *ins-2* (GT_5_101747) seeds; Dr. Yunde Zhao (University of California, San Diego) for providing *yuc4/6* seeds; and Dr. Yuxin Hu (Institute of Botany, Chinese Academy of Sciences) for providing *trp2-301* seeds. We also thank Dr. Weicai Yang and Dr. Hongju Li (Institute of Genetics and Developmental Biology, Chinese Academy of Sciences) for technical assistance in embryo observation and Dr. Steven M. Smith (The University of Western Australia) for critical reading of the manuscript. This work was supported by the National Natural Science Foundation of China (Grants 91117001, 91117016, and 30830009).

1. Wang R, Estelle M (2014) Diversity and specificity: Auxin perception and signaling through the TIR1/AFB pathway. *Curr Opin Plant Biol* 21:51–58.
2. Teale WD, Paponov IA, Palme K (2006) Auxin in action: Signalling, transport and the control of plant growth and development. *Nat Rev Mol Cell Biol* 7(11):847–859.
3. Kieffer M, Neve J, Kepinski S (2010) Defining auxin response contexts in plant development. *Curr Opin Plant Biol* 13(1):12–20.
4. Zhao Y (2012) Auxin biosynthesis: A simple two-step pathway converts tryptophan to indole-3-acetic acid in plants. *Mol Plant* 5(2):334–338.
5. Woodward AW, Bartel B (2005) Auxin: Regulation, action, and interaction. *Ann Bot (Lond)* 95(5):707–735.
6. Tao Y, et al. (2008) Rapid synthesis of auxin via a new tryptophan-dependent pathway is required for shade avoidance in plants. *Cell* 133(1):164–176.
7. Stepanova AN, et al. (2008) TAA1-mediated auxin biosynthesis is essential for hormone crosstalk and plant development. *Cell* 133(1):177–191.
8. Zhao Y, et al. (2001) A role for flavin monooxygenase-like enzymes in auxin biosynthesis. *Science* 291(5502):306–309.
9. Tivendale ND, Ross JJ, Cohen JD (2014) The shifting paradigms of auxin biosynthesis. *Trends Plant Sci* 19(1):44–51.
10. Ouyang J, Shao X, Li J (2000) Indole-3-glycerol phosphate, a branchpoint of indole-3-acetic acid biosynthesis from the tryptophan biosynthetic pathway in *Arabidopsis thaliana*. *Plant J* 24(3):327–333.
11. Normanly J, Cohen JD, Fink GR (1993) *Arabidopsis thaliana* auxotrophs reveal a tryptophan-independent biosynthetic pathway for indole-3-acetic acid. *Proc Natl Acad Sci USA* 90(21):10355–10359.
12. Wright AD, et al. (1991) Indole-3-acetic acid biosynthesis in the mutant maize *orange pericarp*, a tryptophan auxotroph. *Science* 254(5034):998–1000.
13. Baldi BG, Maher BR, Slovin JP, Cohen JD (1991) Stable isotope labeling, in vivo, of D- and L-tryptophan pools in *Lemna gibba* and the low incorporation of label into indole-3-acetic acid. *Plant Physiol* 95(4):1203–1208.
14. Last RL, Fink GR (1988) Tryptophan-requiring mutants of the plant *Arabidopsis thaliana*. *Science* 240(4850):305–310.
15. Radwanski ER, Barczak AJ, Last RL (1996) Characterization of tryptophan synthase alpha subunit mutants of *Arabidopsis thaliana*. *Mol Gen Genet* 253(3):353–361.
16. Last RL, Bissinger PH, Mahoney DJ, Radwanski ER, Fink GR (1991) Tryptophan mutants in *Arabidopsis*: The consequences of duplicated tryptophan synthase beta genes. *Plant Cell* 3(4):345–358.
17. Zhang R, Wang B, Ouyang J, Li J, Wang Y (2008) *Arabidopsis* indole synthase, a homolog of tryptophan synthase alpha, is an enzyme involved in the Trp-independent indole-containing metabolite biosynthesis. *J Integr Plant Biol* 50(9):1070–1077.
18. Capron A, Chatfield S, Provart N, Berleth T (2009) Embryogenesis: Pattern formation from a single cell. *Arabidopsis Book* 7:e0126.
19. Lau S, Slane D, Herud O, Kong J, Jürgens G (2012) Early embryogenesis in flowering plants: Setting up the basic body pattern. *Annu Rev Plant Biol* 63:483–506.
20. Friml J, et al. (2003) Efflux-dependent auxin gradients establish the apical-basal axis of *Arabidopsis*. *Nature* 426(6963):147–153.
21. Blilou I, et al. (2005) The PIN auxin efflux facilitator network controls growth and patterning in *Arabidopsis* roots. *Nature* 433(7021):39–44.
22. Cheng Y, Dai X, Zhao Y (2007) Auxin synthesized by the YUCCA flavin monooxygenases is essential for embryogenesis and leaf formation in *Arabidopsis*. *Plant Cell* 19(8):2430–2439.
23. Miles EW (1991) Structural basis for catalysis by tryptophan synthase. *Adv Enzymol Relat Areas Mol Biol* 64:93–172.
24. Radwanski ER, Zhao J, Last RL (1995) *Arabidopsis thaliana* tryptophan synthase alpha: Gene cloning, expression, and subunit interaction. *Mol Gen Genet* 248(6):657–667.
25. Petersson SV, et al. (2009) An auxin gradient and maximum in the *Arabidopsis* root apex shown by high-resolution cell-specific analysis of IAA distribution and synthesis. *Plant Cell* 21(6):1659–1668.
26. Barlier I, et al. (2000) The *SUR2* gene of *Arabidopsis thaliana* encodes the cytochrome P450 CYP83B1, a modulator of auxin homeostasis. *Proc Natl Acad Sci USA* 97(26):14819–14824.
27. Hamann T, Benkova E, Bäurle I, Kientz M, Jürgens G (2002) The *Arabidopsis BODENLOS* gene encodes an auxin response protein inhibiting MONOPTEROS-mediated embryo patterning. *Genes Dev* 16(13):1610–1615.
28. Hardtke CS, Berleth T (1998) The *Arabidopsis* gene *MONOPTEROS* encodes a transcription factor mediating embryo axis formation and vascular development. *EMBO J* 17(5):1405–1411.
29. Mayer U, Buttner G, Jurgens G (1993) Apical-basal pattern formation in the *Arabidopsis* embryo: Studies on the role of the *gnom* gene. *Development* 117(1):149–162.
30. Szemenyei H, Hannon M, Long JA (2008) TOPLESS mediates auxin-dependent transcriptional repression during *Arabidopsis* embryogenesis. *Science* 319(5868):1384–1386.
31. Li J, Last RL (1996) The *Arabidopsis thaliana trp5* mutant has a feedback-resistant anthranilate synthase and elevated soluble tryptophan. *Plant Physiol* 110(1):51–59.
32. Strader LC, et al. (2011) Multiple facets of *Arabidopsis* seedling development require indole-3-butyric acid-derived auxin. *Plant Cell* 23(3):984–999.
33. Mou Z, He Y, Dai Y, Liu X, Li J (2000) Deficiency in fatty acid synthase leads to premature cell death and dramatic alterations in plant morphology. *Plant Cell* 12(3):405–418.
34. Gray WM, Ostin A, Sandberg G, Romano CP, Estelle M (1998) High temperature promotes auxin-mediated hypocotyl elongation in *Arabidopsis*. *Proc Natl Acad Sci USA* 95(12):7197–7202.
35. Sun X, et al. (2014) An in-advance stable isotope labeling strategy for relative analysis of multiple acidic plant hormones in sub-milligram *Arabidopsis thaliana* seedling and a single seed. *J Chromatogr A* 1338:67–76.
36. Fu J, Chu J, Sun X, Wang J, Yan C (2012) Simple, rapid, and simultaneous assay of multiple carboxyl containing phytohormones in wounded tomatoes by UPLC-MS/MS using single SPE purification and isotope dilution. *Anal Sci* 28(11):1081–1087.